THREE-DIMENSIONAL FLUX PREDICTION FOR A DISH CONCENTRATOR CAVITY RECEIVER

Greg Burgess[1], José Zapata[2], Rémi Chauvin[3], Mark Shortis[4], John Pye[5] and Jessica Preston[6]

[1] BSc(Hons), MAppSc, Research Officer, Research School of Engineering (RSE), Australian National University (ANU), Canberra, ACT, 0200, Australia, Phone: +61 2 6125 5130, greg.burgess@anu.edu.au.

[2] BEng(Hons), PhD student, RSE, ANU.

[3] BEng, Occupational Trainee, RSE, ANU.

[4] Professor, School of Mathematical and Geospatial Sciences, RMIT University, GPO Box 2476 Melbourne 3001, Australia

[5] BE(Hons)/BSc, PhD, Lecturer, RSE, ANU.

[6] BSc (Eng), MSc (Eng), Engineer.

Abstract

This paper describes the development of ray tracing models for a 500 m^2 dish concentrator. Two distinct types of model have been created: (1) a model in OptiCAD based on the generic dish design, which uses design values for mirror facet geometry, and averaged values for mirror facet slope and pointing error; (2) a model in Tonatiuh which incorporates measured values of these parameters, for the prototype dish completed in 2009. In both cases the goal is accurate prediction of the three-dimensional flux distribution in the focal region, in particular as an aid to receiver design.

Inputs to the ray tracing models have included photogrammetry, flux mapping and Finite Element Analysis. Photogrammetry was primarily used to measure mirror panel geometry prior to installation on the dish, and mirror panel pointing error on the completed dish. On-sun flux mapping of the image produced by individual mirror panels gave information on panel slope error. The image of the moon created by the complete dish on a planar target gave a two-dimensional flux distribution which was used to calibrate the ray tracing models.

The methodologies used can with suitable modification also be employed on other concentrator systems, such as heliostat / central receiver.

Keywords: Dish; ray tracing; photogrammetry; flux mapping;

1. Introduction

The design of a cavity receiver for a dish concentrator must take into account factors such as heat transfer to the receiver working fluid, avoidance of hot spots on the receiver surface, and minimization of radiative and convective heat losses. Knowledge of the three-dimensional flux distribution in the focal region is important in all of these areas. In particular, the flux distribution on the heat transfer tubes or surfaces, for a particular cavity geometry, affects the temperature distribution on the cavity walls, and the location of the boiling region in a steam receiver [1][2].

Measurement of the three dimensional flux distribution of a high accuracy dish concentrator is challenging experimentally [3], and does not provide information about the effect of concentrator or receiver design changes, or concentrator manufacturing variability. Measurement of the two dimensional flux distribution in the focal plane is simpler, but does not provide detailed information on the flux profile within a cavity receiver. For these reasons flux prediction via ray tracing has been preferred at the Australian National University (ANU).

This paper describes the development of ray tracing models for the 'Generation II Big Dish', a 500 m^2 dish concentrator design. The first prototype of the design, known as 'SG4', was constructed at the ANU campus in 2009 (fig. 1) [4]. The concentrator consists of 380 individual mirror facets mounted on a front surface mesh of rolled steel, which is in turn supported by a space frame structure. Two distinct classes of model have been created: firstly, models of the generic dish design, in which averaged values are applied to parameters such as mirror facet slope and pointing error; and, secondly, models of the as-built SG4

concentrator, incorporating the measured or estimated values of these parameters for individual mirror panels. The outputs of both types of model have been compared to measurements of the SG4 flux distribution on a planar target.

Fig. 1: Rear view of SG4 dish, showing space frame structure and square mirror facets.

The development of the ray tracing models incorporated as inputs: (i) the design values of the mirror facet locations and orientations, (ii) photogrammetry, (iii) flux mapping, and (iv) Finite Element Analysis. These are described in the sections below.

2. Ray tracing model parameters

OptiCAD (v7 and v10) was used for the ray tracing model of the Generation II dish design. The open-source ray-tracing program Tonatiuh v1.2.6 [5] has also been used, primarily for a detailed SG4 model. A Tonatiuh model using averaged dish properties was also created, for the purpose of cross-comparison with the OptiCAD ray tracing. The parameters needed for a complete ray tracing model of a faceted dish are given in Table 1.

The OptiCAD Generation II ray tracing model represents mirror facets as spherical segments, with radius of curvature equal to the design value for the dish region. Initial values of average panel pointing and slope error were derived from jig photogrammetry and panel flux mapping (both described below). The predicted peak and geometric concentration ratios were, however, both higher than given by the measured SG4 flux distribution. The model was then iteratively refined by ad-hoc increases in the pointing and slope error until a good match was made with the flux distribution. The need to increase these error parameters can be understood in terms of the completed space frame structure having position errors larger than those of the jig.

The detailed SG4 model in Tonatiuh incorporates the measured profiles and pointing errors of all 380 individual mirror panels. The model also allows for the deformation of the panel profile which occurs when the panel is mounted on the dish, and for panel asphericity and orientation. Panel pointing errors were determined by measurement of the completed dish surface using photogrammetry. This measurement confirmed that the dish structure has larger deviations from the ideal paraboloid than the construction jig.

Parameter	Generic Generation II dish design models	SG4 models
Panel centre location	Design location	Design location[1]
Panel pointing direction	Initial value: Design direction plus random pointing error, with magnitude taken from jig photogrammetry	Pointing direction for each panel measured using photogrammetry.
Panel unloaded curvature	Spherical panels with design curvatures in three bands, corresponding to inner, middle and outer regions of the dish.	Elliptic paraboloid sections with biaxial radii of curvature fitted to individually measured panel surface profiles.
Panel slope error	Initial value: Average panel slope error as measured by flux mapping and photogrammetry	Average panel slope error as measured by flux mapping and photogrammetry[2]
Effect of panel mounting on panel curvature	Not taken into account	Panel biaxial radii of curvature adjusted according to Strand7 FEA predictions

Table 1. Dish ray tracing model input parameters, specified for the Generation II Big Dish design and the as-built SG4 concentrator.

2.1 Design parameters

The Generation II design utilizes the common approach in dish and solar furnace construction of spherical mirror elements mounted on a paraboloidal substrate [6][7]. Without any change in the structure, concentrators based on the design can be assembled using varying numbers of panel radii of curvature (R.O.C.), ranging from a single uniform value [8], up to three or more distinct radii of curvature. The constructed SG4 dish uses mirror facets in three ranges of radius of curvature, corresponding to facet location in either the inner, middle or outer region of the dish.

2.2 Photogrammetry

Photogrammetry is a well-established technique for deriving accurate spatial coordinates of reference points (targets) from camera images taken from different viewpoints and with varied camera orientation [9]. Photogrammetry is configurable in terms of the size of the object, the spatial density of the locations measured and the accuracy of the derived 3D coordinates. The geometric analysis of solar concentrators based on photogrammetric measurement has been previously described in Refs. [10][11][12]. Photogrammetry was used throughout the SG4 dish development and construction [13]. A Nikon D300 and a Nikon D300s camera were used for image capture; processing of the images was carried out with VMS (Vision Measurement System). At a moderate cost, photogrammetry provided a means of efficiently measuring the assembly of the dish structure, performing quality control of mirror panel fabrication, and, finally, validating the mirrored front surface to a spatial accuracy of ±0.3 mm. These three applications, and their relationship to the development of dish ray tracing models, are discussed below.

[1] The flux distribution produced by a mirror facet is relatively insensitive to an offset of the mirror position in the plane of the paraboloid.

[2] It would be possible to apply the individual panel slope errors as measured by photogrammetry; however this was considered an unwarranted level of detail.

1) Measurement of the jig structure on which the concentrator was assembled gave an initial estimate of panel RMS pointing error. The jig support points were adjusted to an RMS deviation of ±0.6 mm from the true paraboloid. A random local height error of this magnitude at mirror facet corners translates to an RMS pointing error of approximately 1 mrad; this value was initially used in the Generation II ray tracing models. This was expected (and later confirmed) to be an optimistic estimate, as some spring back or deformation of the dish structure inevitably occurs when it is released from the jig.

2) Measurement of individual mirror panels (before installation on the dish) was used to determine their best-fit geometry (modeled as an elliptic paraboloid, to allow for possible facet asymmetry) and slope error.

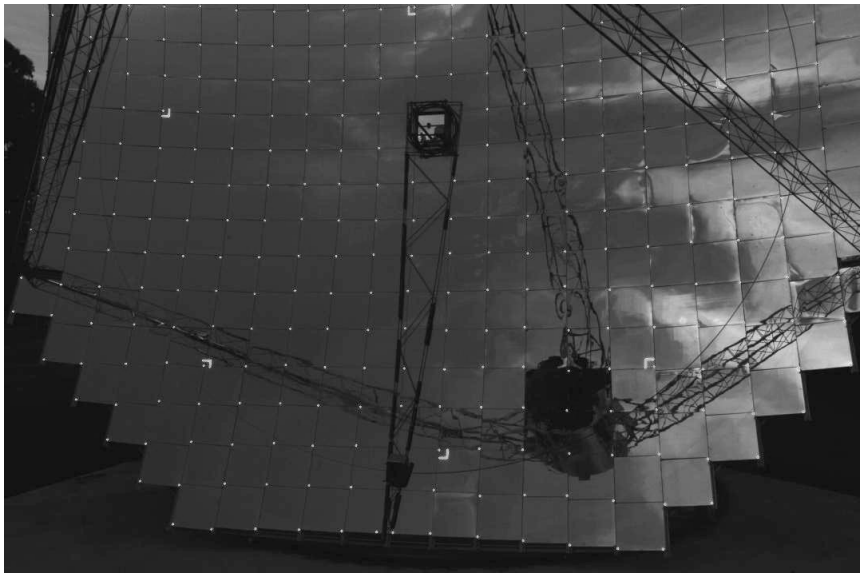

Fig. 2: Camera image with flash of SG4 dish with retro reflective targets located at panel corners.

Detailed measurement of a mirrored surface using photogrammetry is time consuming, as the mirror surface must either be painted to make it opaque, or an array of adhesive targets must be applied manually. Instead the mirror panels were characterized by using a data projector to create a dense array of targets on the metal rear surface of the panel. The rear surface profile was shown to be a close match to that of the mirrored surface, other than in the edge region and also in respect of any imperfections in the mirror itself.

Mirror panel slope error (resolved into orthogonal components) was calculated by computing the local normals to the planes formed by triangular sets of targets. The local normals were compared to either the best fit geometry (in which case they essentially gave a measure of medium scale geometric deformities in the panel), or to a surface corresponding to the installed location of the panel on the dish paraboloid, or to the desired radius of curvature (in which cases they also represented larger scale deviations). The photogrammetry target spacing was 25 – 30 mm, which, along with the measurement precision of 15-20 μm in the axis orthogonal to the plane of the panel, limited the absolute accuracy of the slope error calculation (which was originally developed as a quality control measure). Fitting of a parametric surface to the point cloud formed by the targets may yield some improvement [14], but the use of the panel rear surface is a fundamental limitation.

A deflectometry system for measuring the geometry and slope error of dish mirror facets has also been developed at ANU [15]. It would give a more detailed profile of the reflective surface than photogrammetry, but was incomplete and not implemented during SG4 mirror panel production.

3) Measurement of the completed dish yielded the pointing error of individual mirror facets in place on the dish (fig. 2). Retro reflective targets were placed as near as possible to the junctions between adjacent mirror panels. The local height deviation from the ideal paraboloid was assumed to be identical for the adjacent corners of each group of four mirror panels. The panel pointing errors were incorporated into the Tonatiuh SG4 model.

2.3 Flux Mapping

For both dish and individual panel flux-mapping the camera-target method [3][16] was used. Images were captured in 12 bit grayscale resolution with a Prosilica GC1290M camera. Custom written routines in IDL (Interactive Data Language) were used for processing the images. Mirror panels were flux mapped on-sun, whilst the moon was used as the light source for dish flux maps.

Scaling was performed by integrating the pixel grayscale values over the area of the target and assuming that all of the reflected flux fell within the target region. This is a possible source of error as if there is an unknown amount of spillage outside the target region the distribution will be incorrectly scaled (the peak will be over-estimated). Background light and camera sensor levels were removed by capturing an image with the concentrator (dish or mirror panel) pointing away from the light source; this image was subtracted from the live image before processing.

2.3.1 Individual panel flux mapping

On-sun flux distributions were obtained for a limited number of mirror facets before installation on the dish surface (fig. 3). On-sun characterization provides direct visual evidence of mirror panel optical quality, as well as giving quantitative values for parameters such as power in radius and panel slope error.

Panels were flux mapped using the configuration shown in fig. 3. In general the angle θ was significantly larger than zero, i.e. the sun was well above the horizon. The flux distribution formed at the target is the same as would occur with the panel located at angular position θ on a paraboloid, if the distance r from the reflection point to the focal point is the same as the mirror-target distance L (see fig. 4)[3]. The target image is therefore the convolution of the sunshape distribution and the mirror facet slope errors relative to the segment at point P of a perfect paraboloid.

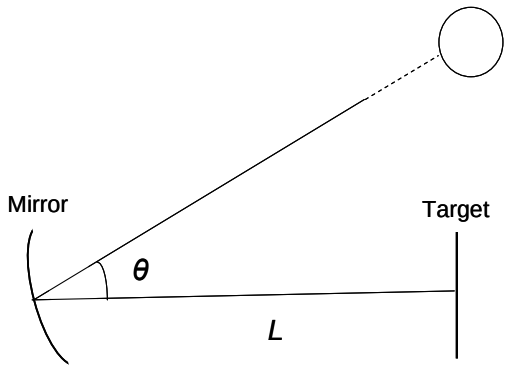

Fig. 3: Configuration for mirror panel flux mapping

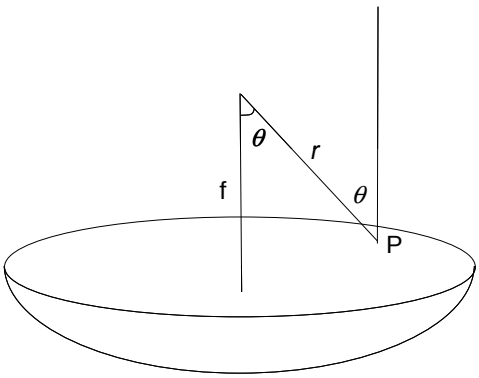

Fig. 4: Equivalent situation on dish paraboloid

The target distance L was in general varied through 0.5 m steps around the position which gave the best quality image. The mirror panel slope error components for a given θ and L were obtained by first fitting a bivariate Gaussian distribution to the processed image, then deconvoluting to remove the effect of the sunshape. The approximation of a Gaussian sunshape (valid as a single mirror panel has relatively low concentration [17]) was used to reduce computation time. The minimum value of the slope error components was typically of the order of 1 mrad, which was in general agreement with estimations from photogrammetry [13]. It was subsequently found that applying a slope error of 1.5 mrad to all mirror panels, in the OptiCAD Generation II ray tracing model gave a better match to the measured optics of the completed dish (see

[3] The target in fig. 3 is actually orthogonal to the incident light, whilst in fig. 4 the flux distribution would usually be measured on a planar target perpendicular to the axis of the paraboloid. However as the angle subtended by the panel from distance L is relatively small, the distributions would (to a close approximation) only differ by that on the fig. 3 target by being stretched by a factor $1/(\cos\theta)$ along one axis.
r and θ are related by the polar equation of a parabola: $r = 2f\,(1+\cos\theta)^{-1}$

Section 2.3.2). This occurs as mirror panels are only placed in one of three regions on the dish, demarcated by panel R.O.C., rather than (in general) being placed at the position corresponding to the minimum slope error (θ,r) pair.

In some cases mirror panels had a significant asymmetry, identified by photogrammetry, with differing radii of curvature along orthogonal axes through the panel centre. The asymmetry will increase or decrease astigmatic effects, according to whether the larger R.O.C. axis of the panel is aligned with the sun-mirror-target plane. As mirror panels are mounted with their edges along parallel rails (Fig. 1), they cannot in general be oriented in the ideal position which would *minimize* astigmatism. However of the two possible orientations for a given panel, it is possible to choose the one which would at least *reduce* astigmatic effects, with a possible net gain for the dish optical quality [18].

2.3.2 Dish lunar flux mapping

Flux mapping of the 57 m^2 Eurodish and DISTAL II concentrators, with peak flux of the order of 12,000 kW/m^2 was successfully carried out by Ulmer et al using a water cooled target [16]. SG4 would however require an expensive, proportionally larger target, and the previously demonstrated approach of lunar imaging was used [4][19][20][4]. The flux distribution produced on a planar target (fig. 5) was used to calibrate the ray tracing models.

The cost benefit of lunar flux mapping must be weighed against a number of disadvantages, including: operation is only possible on a few nights per month with near full moon conditions; the flux distribution cannot be measured in the full range of conditions which prevail in on-sun operation (e.g. ambient temperature and sun elevation)[5]; the acquired images must be corrected for the difference between the lunar angular diameter (at the time of the test) and the conventional solar diameter, which can differ by up to 7%.

Open loop tracking is employed on the SG4 dish, incorporating a sun position algorithm developed by Grena [22]. In order to track the moon on a given night, the date and time which most gave a sun position as near as possible to the moon position was determined and entered into the controller. Manual offsets were then applied to more accurately shift the lunar image to the centre of the target. The offsets were adjusted approximately every 15 minutes, to correct for the different trajectories of the lunar and solar paths. Images were obtained with the target moved in 0.1 m steps along the dish axis; the image with the best optics, which occurred close to the design focal length of 13.4 m, was used for detailed analysis.

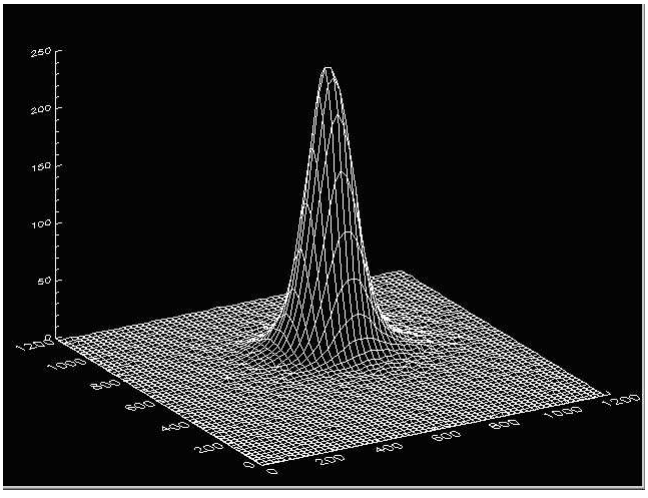

Fig. 5: Surface plot (unscaled) of the lunar flux distribution of SG4 dish, measured 4 September 2009. At the time of image capture the moon was 97.6% full and had an angular radius of 4.35 mrad.

[4] The earlier 400 m^2 SG3 Big Dish was also flux mapped on-sun, however it had a peak flux of less than 1,500 kW/m^2 [21].

[5] This was also the case with the dish flux mapping by Ulmer et al, which had to be carried out in late afternoon, in less than 'full sun' conditions', to avoid discoloration of the Al_2O_3 coated target surface.

The flux distribution in the focal plane represents the convolution of the light source and the dish optical errors; it is therefore not possible to carry out a simple linear correction to the lunar generated image to predict the on-sun flux distribution. Corrected values for the parameters of interest (the geometric and peak concentration ratios) were instead obtained by comparing the outputs of OptiCAD models with a standard sunshape light source to models using a light source with the lunar angular diameter (4.35 mrad) at the time of the test[6]. This yielded corrections of approximately -1% and -3% to the geometric and peak concentration ratios respectively. These adjustments are specific to a particular moon angular diameter and to the SG4 dish optics.

Applying the above corrections, as well as a correction relating to target non-Lambertian reflectance (see Section 2.3.3) gave the following optical parameters for SG4:

- Peak concentration: 14,100 suns
- Geometric concentration ratio (90% capture): 3,900
- Geometric concentration ratio (95% capture): 2,240

The 95% capture ratio concentration is the least robust of these parameters as it is requires integration into the low intensity region of the image, which makes it most sensitive to any error in the removal of light and camera sensor background levels.

2.3.3 Target reflectance properties

The preferred coating for a flux mapping target is a material such as Al_2O_3, which has near-Lambertian reflectance properties. To date, however, the targets used have been coated with a matt white paint which shows significant deviation from Lambertian reflectance (e.g. ~20% reduction in reflectance for source or reflected light at 50° to the normal). However for mirror panel flux mapping the error introduced in the measured light levels, compared to the actual target irradiance, is kept small as (i) the target subtends a small angle from the target distance, (ii) a telephoto lens was used on the camera in order to minimize the field of view angle.

In the case of the dish flux mapping the use of a non-Lambertian target has a (prima facie) more significant effect, due to the wider range of angles made by the reflected light on the target surface. The effect of the target reflectance properties was simulated in a ray tracing model: for a mirror panel located at angular position θ the mirror reflectance in the ray tracing model was reduced by the measured decrease in target reflectance at the corresponding angle. The resulting effect on the key flux distribution parameters, relative to a true Lambertian target, was quite small, with increases in peak and 95% capture geometric concentrations of 2.5% and 1.0% respectively[7]. The negatives of these values were then applied as corrections.

2.4 Finite Element Analysis

Strand7 FEA software was used to predict the deformations which occur when mirror panels are mounted on the dish structure. Each panel is glued to lightweight rolled rails (which match the curvature of the paraboloid) along two edges. The complexity involved in setting up the point contact boundary conditions makes it impractical to analyze all relevant combinations of panel and rail curvature. However based on analysis of representative cases, it was found (as might be expected) that the mirror facet radius of curvature approximately matches the paraboloid along the mounted axis, but stays near its free value on the other axis. This has been incorporated into the Tonatiuh SG4 ray tracing model, whilst the OptiCAD Generation II model makes no allowance for mounting effects. The FEA predictions could be tested using photogrammetry of installed mirror panels, but this has not been done to date.

---

[6] The moon was 97.6% full; the deviation from circularity was not incorporated into the model.

[7] The concentrations show an apparent *increase* as the reduced reflectance at angles away from the normal effectively reduces the weighting of outer region mirror panels, which will in general produce a larger sized image in the focal plane.

3. Ray tracing model receiver flux predictions

The OptiCAD Generation II design model shows a central band of high flux within the center of the cylindrical section of the cavity receiver (fig. 6, top left). The fluid absorbs the greatest amount of energy within this region, as shown in fig. 6, bottom left. Most of the boiling region of the steam receiver is in this section; the steam is superheated further into the cavity.

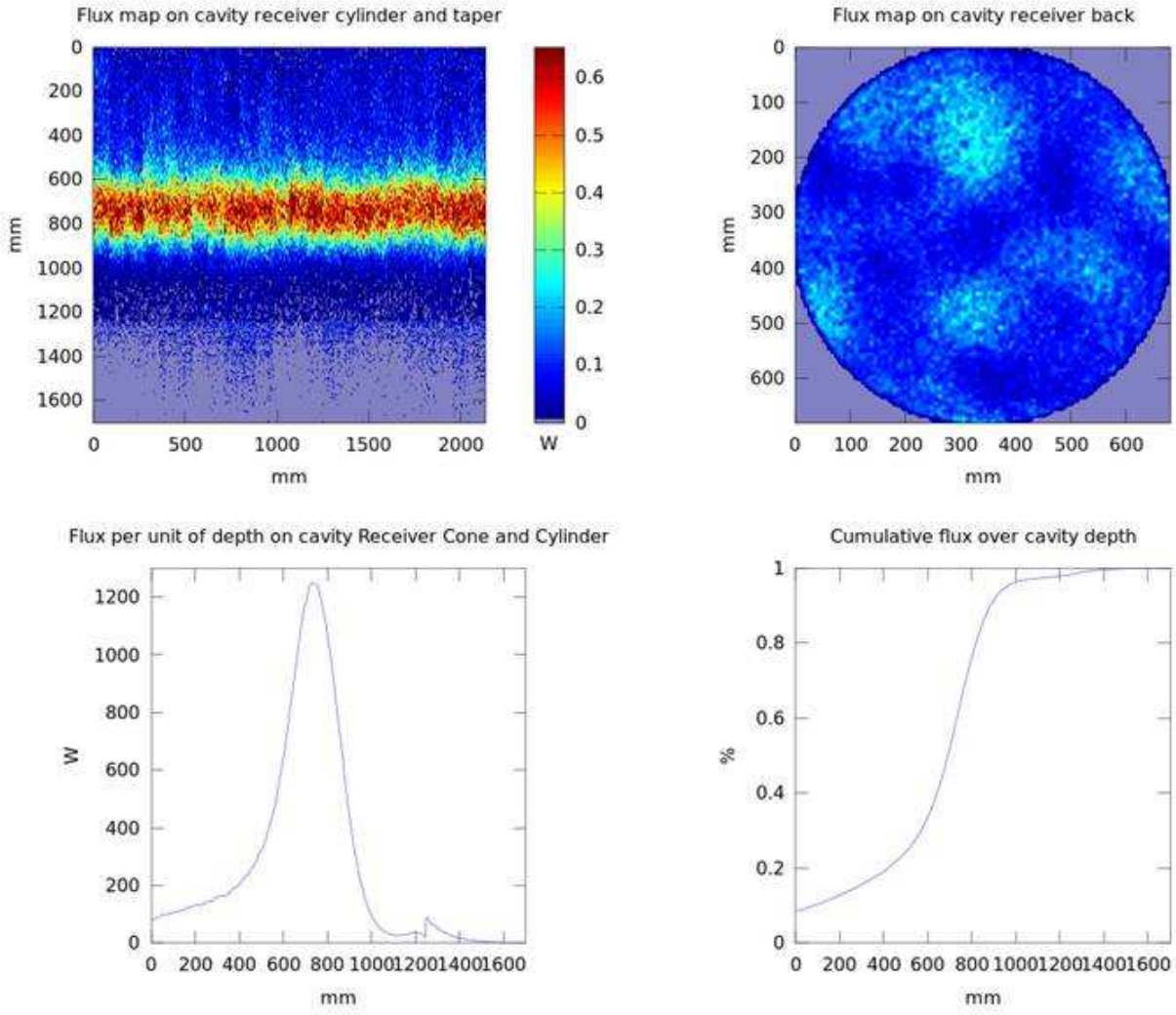

Fig. 6: Outputs from OptiCAD ray tracing model: (top left) flux on inside walls of the cylindrical receiver cavity; (top right) flux at the back section of the receiver; (bottom left) flux intensity on 1 mm wide x 2.25 m long strips of the receiver cavity wall. The 1 mm increments run parallel to the cylindrical receiver axis (0 mm = back of the receiver; 1600 mm = aperture); (bottom right) cumulative flux on the receiver walls, from the back (0 mm) to the aperture (1600 mm). The starting value is non-zero as some radiation is incident upon and absorbed by tubes at the back of the cavity.

When observed by eye, the flux distribution at the entrance to the receiver cavity shows a noticeable asymmetry (fig. 7, left), which is not predicted by the Generation II dish design model. The more realistic Tonatiuh SG4 model qualitatively reproduces this asymmetry (fig. 7, right), which provides preliminary confirmation of its accuracy. In both the fig. 7 camera image and the Tonatiuh generated contour plot, a range compression curve has been applied, which enhances low brightness levels (as occurs with the human eye). This increases the apparent power contained in the spillage, which is not obvious in the linear ‘machine vision’ images used for flux mapping.

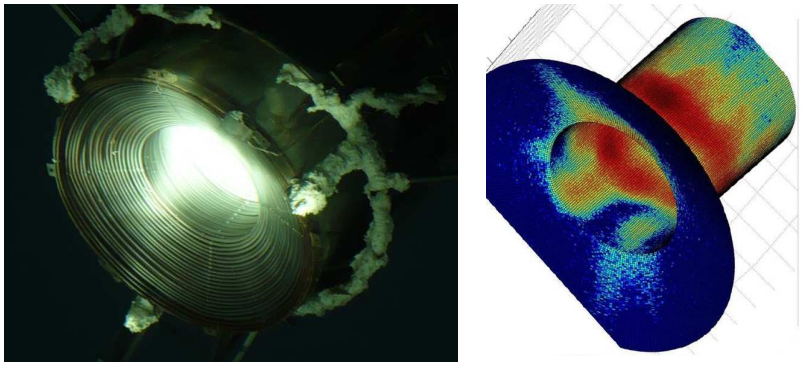

Fig. 7: (Left) Camera image of the SG4 dish steam receiver on sun. (Right) contour plot of flux distribution on the receiver surface generated by Tonatiuh ray tracing.

4. Conclusion

To date flux mapping of the image created by the complete dish concentrator has only been carried out using the moon as a light source, and on a planar target. Future plans include using an infra-red camera for analysis of the temperature within the receiver during on-sun operation, and measurement of the (lunar) flux at selected locations within the receiver cavity. Both of these approaches will be used for further validation and refinement of the ray tracing models. Further work also remains to be done in quantifying the agreement between the SG4 ray tracing model and the measured planar flux distribution.

Thanks to the techniques, measurements and effort put into this area of research, it is now possible to determine the influence of parabolic dish concentrator construction materials and methods, as well as changes in receiver geometry in the distribution of incoming flux on a cavity receiver.

Acknowledgements

The Generation II dish design was developed by ANU and Wizard Power personnel, using funding from Wizard Power and the Australian Commonwealth Government. Other sources of funding for the work described in this paper include the Australian Solar Institute, Australian Postgraduate Awards, and ANU.

References

[1] G Burgess, K Lovegrove, S Mackie, J Zapata and J Pye, (2011). Direct steam generation using the SG4 500m² paraboloidal dish concentrator, Proceedings of SolarPACES 2011, Granada, September 2011.

[2] J Zapata, J Pye and K Lovegrove, (2011). Dynamic simulation of mono-tube cavity receivers for direct steam generation, Proceedings of SolarPACES 2011, Granada, September 2011.

[3] J Ballestrín, G Burgess and J Cumpston. Heat flux and high temperature measurement technologies for concentrating solar power (CSP). In: Concentrating solar power technology - developments and applications. Ed. K Lovegrove and W Stein. Woodhead Publishing (In press).

[4] K Lovegrove, G Burgess and J Pye. A new 500 m² paraboloidal dish solar concentrator. Solar Energy, 85 (2011), 620-626.

[5] http://tonatiuhchronicles.blogspot.com/

[6] JPL (Jet propulsion Laboratory), (1980). Proceedings of the First Semi-Annual Distributed Receiver Systems Program Review. DOE/JPL–1060–33, Pasadena, CA: Jet Propulsion Laboratory. April 1980.

[7] L Jaffe. Test results on parabolic dish concentrators for solar thermal power systems. Solar Energy, 42 (1989) 173-187.

[8] G Johnston, K Lovegrove and A Luzzi. Optical performance of spherical reflecting elements for use with paraboloidal dish concentrators. Solar Energy 74 (2003) 133-140

[9] T Luhmann, S Robson, S Kyle, I Harley, (2006). Close range photogrammetry : principles, techniques and applications. Whittles Publishing, Caithness, UK.

[10] K Pottler, E Lüpfert, G Johnston, M Shortis. Photogrammetry: A powerful tool for geometric analysis of solar concentrators and their components. Journal of Solar Energy Engineering, 127 (2005) 94-101.

[11] M Shortis and G Johnston. Photogrammetry: An available surface characterisation tool for solar concentrators. Part 1: Measurement of surfaces. Jnl of Solar Energy Engineering, 118 (1996) 146-150.

[12] M Shortis and G Johnston. Photogrammetry: An available surface characterisation tool for solar concentrators. Part 2: Assessment of surfaces. Jnl of Solar Energy Engineering, 119 (1997) 286-291.

[13] M Shortis and G Burgess. Photogrammetric Monitoring of the Construction of a Solar Energy Dish Concentrator. Photogrammetric Engineering and Remote Sensing, 78 (2012) 519-527.

[14] J Roca-Pardiñas, H Lorenzo, P Arias, and J Armesto, J.. From laser point clouds to surfaces: Statistical nonparametric methods for three-dimensional reconstruction. Computer-Aided Design, 40 (2008) 646-652

[15] P Scott and G Burgess (2010). Measurement of mirror panels using coloured-pattern deflectometry, Proceedings of SolarPACES 2010, Perpignan, France, September 2010.

[16] Ulmer S, Wolfgang R, Heller P, Lüpfert E, Beam Characterization and Improvement with a Flux Mapping System for Dish Concentrators. Journal of Solar Energy Engineering, 124 (2002) 182-188.

[17] P Bendt and A Rabl. Optical analysis of point focus parabolic radiation concentrators. Applied Optics 20 (1991) 674-683.

[18] G Burgess, P Scott and J Pye (2008). Spherical and asymmetric mirror panels for paraboloidal concentrators. ISES-AP 2008 (3rd International Solar Energy Society Conference, Asia Pacific region, 46th ANZSES Conference), Sydney, November 2008.

[19] S. Biryukov. Determining the optical properties of PETAL, the 400 m2 parabolic dish at Sede Boqer. Journal of Solar Energy Engineering, 126 (2004), 827–832.

[20] P Siangsukone, G Burgess and K Lovegrove (2004). Full Moon Flux Mapping the 400m2 'Big Dish' at the Australian National University. Proceedings of the 42nd ANZSES Conference, Perth, 1–3 December 2004.

[21] G Johnston. Flux Mapping the 400 m "Big Dish" at the Australian National University. Journal of Solar Energy Engineering, 117 (1995), 290-293.

[22] R Grena. An algorithm for the computation of the solar position. Solar Energy, 42 (2008), 462-470.